Programmed transfer of sequence information into molecularly imprinted polymer (MIP) for hexa(2,2'-bithien-5-yl) DNA analog formation towards single nucleotide polymorphism (SNP) detection

Journal:	*ACS Applied Materials & Interfaces*
Manuscript ID	am-2016-14340x
Manuscript Type:	Article
Date Submitted by the Author:	09-Nov-2016
Complete List of Authors:	Bartold, Katarzyna; Institute of Physical Chemistry of the Polish Academy of Sciences Pietrzyk-Le, Agnieszka; Institute of Physical Chemistry of the Polish Academy of Sciences, Department of Physical Chemistry of Supramolecular Complexes Huynh, Tan-Phat; Institute of Physical Chemistry of the Polish Academy of Sciences Iskierko, Zofia; Polska Akademia Nauk Instytut Chemii Fizycznej Sosnowska, Marta; Institute of Physical Chemistry of the Polish Academy of Sciences Noworyta, Krzysztof; Institute of Physical Chemistry of the Polish Academy of Sciences Lisowski, Wojciech; Institute of Physical Chemistry, Polish Academy of Sciences Sannicolo, Francesco; Universita' di Milano, Dipartimento di Chimica and CIMAINA Cauteruccio, Silvia; University of Milan, Department of Chemistry Licandro, Emanuela; Univeristy of Milan, Department of Organic and Industrial Chemistry D'Souza, Francis; University of North Texas,, Department of Chemistry Kutner, Wlodzimierz; Institute of Physical Chemistry of the Polish Academy of Sciences, Department of Physical Chemistry of Supramolecular Complexes

Programmed transfer of sequence information into molecularly imprinted polymer (MIP) for hexa(2,2'-bithien-5-yl) DNA analog formation towards single nucleotide polymorphism (SNP) detection

Katarzyna Bartold,[a] *Agnieszka Pietrzyk-Le,*[a,*] *Tan-Phat Huynh,*[a,b] *Zofia Iskierko,*[a] *Marta Sosnowska,*[a,b] *Krzysztof Noworyta,*[a] *Wojciech Lisowski,*[a] *Francesco Sannicolò,*[c] *Silvia Cauteruccio,*[c] *Emanuela Licandro,*[c] *Francis D'Souza,*[b,*] *and Wlodzimierz Kutner*[a,d,*]

[a] Institute of Physical Chemistry, Polish Academy of Sciences, Kasprzaka 44/52, 01-224 Warsaw, Poland

[b] Department of Chemistry, University of North Texas, Denton, 1155, Union Circle, #305070 TX 76203-5017, USA

[c] Department of Chemistry, University of Milan, Via Golgi, 19 I-20133 Milan, Italy

[d] Faculty of Mathematics and Natural Sciences, School of Sciences, Cardinal Stefan Wyszynski University in Warsaw, Woycickiego 1/3, 01-938 Warsaw, Poland

KEYWORDS: DNA/RNA analog; PNA; Molecularly imprinted polymer; Bis(2,2'-bithien-5-yl)methane monomer; Oligonucleotide; Capacitive impedimetry; Piezoelectric microgravimetry, Chemosensor

ABSTRACT

A new strategy of simple, inexpensive, rapid, and label-free single nucleotide polymorphism (SNP) detection using robust chemosensors with piezomicrogravimetric (PM), SPR, or capacitive impedimetry (CI) signal transduction is reported. Using these chemosensors, selective detection of a genetically relevant oligonucleotide under FIA conditions within 2 min is accomplished. An invulnerable to non-specific interaction molecularly imprinted polymer (MIP) with electrochemically synthesized probes of hexameric 2,2'-bithien-5-yl DNA analogs discriminating single purine-nucleobase mismatch at room temperature was used. With DFT modeling, synthetic procedures developed, and ITC quantification, adenine (A) or thymine (T) substituted 2,2'-bithien-5-yl functional monomers capable of Watson-Crick nucleobase pairing with the TATAAA oligodeoxyribonucleotide template or its peptide nucleic acid (PNA) analog were designed. Characterized by spectroscopic techniques, molecular cavities, exposed in the MIP, ordered nucleobases on the 2,2'-bithien-5-yl polymeric backbone of the TTTATA hexamer probe designed to hybridize the complementary TATAAA template. That way, an artificial TATAAA-promoter sequence was formed. The purine nucleobases of this sequence are known to be recognized by RNA polymerase to initiate the transcription in eukaryotes. The hexamer strongly hybridized TATAAA with the complex stability constant, $K_s^{\text{TTTATA-TATAAA}} = k_a/k_d \approx 10^6\ \text{M}^{-1}$, as high as that characteristic for longer-chain DNA-PNA hybrids. The CI chemosensor revealed a 5-nM limit of detection, quite appreciable as for the hexadeoxyribonucleotide. The molecular imprinting increased the chemosensor sensitivity to the TATAAA analyte over four times compared to that of the non-imprinted polymer. The herein devised detection platform enabled generating a library of hexamer probes for typing

majority of SNPs as well as studying a molecular mechanism of the complex transcription machinery, physics of single polymer molecules, and stable genetic nanomaterials.

1. Introduction

Inspired by the Watson−Crick double helix,[1, 2] synthetic polymers were explored as templates to direct the polymerization as early as in 1956.[3-5] Then, first investigations of biological macromolecular templates appeared only ten years later.[6] However, the ability to direct polymerization along a template and read the sequence and chain-length information, particularly in the absence of biological catalysts, has remained limited.[4] The self-recognizing and self-organizing properties of biomolecules, and nucleic acids in particular, are exploited to fabricate new nanoscale materials with unique properties and capabilities.[7, 8]

Detection of specific nucleic acid sequences is critical in contemporary biology and medicine. Importantly, there is an increasing interest in personalized medicine in the underlying genetic causes of disease, and this invokes higher demand to detect and identify RNA and DNA sequences.[9] Determination of DNA sequences shows considerable variability between individuals. Most of the variations in the human genome results from single nucleotide polymorphisms (SNPs).[10-13] SNPs are potent molecular genetic markers and valuable indicators for biomedical research, drug development, clinical diagnosis, disease therapy, evolutionary studies, and forensic science.[14-16]

Current methods for SNP genotyping rely on a wide variety of probes, e.g., molecular beacons[17, 18] and nucleic acid analogs.[19-23] So far, several different SNP detection platforms, e.g., fluorescence, gel electrophoresis, mass spectrometry, electrochemistry, and microgravimetry, have been developed. Although they are sensitive, many of them reveal features that limit their

practical use, e.g., tedious assay processes, expensive instruments (e.g., mass spectrometer or a thermal cycler for PCR), or a need for exact control over the experimental conditions (e.g., temperature).[15]

Relatively short oligonucleotide (ON) probes are more sensitive to SNPs because of greater relative impact of a single base-pair mismatch on the hybridization stability of these probes with the target DNA sequence. Short ON probes have superior ability to discriminate SNPs, thus lowering the chance of generating false signals arising from non-specific or non-perfect interactions, characteristic of 15-20 nucleotide hybrids. However, the stability constant of complexes between complementary and target ONs, particularly those containing less than eight nucleotides, depends upon the chain lengths of ONs. No interaction could be detected with thymine- (T) and adenine- (A) oligodeoxyribonucleotides (ODNs) with chain lengths less than five and four nucleotides, respectively[6]. Basically, T- and A-hexadeoxyribonucleotides with two hydrogen bonds of A-T pairs cannot form a stable complex above 0 °C.

Therefore, easily prepared hexamers of DNA analogs capable of hybridizing nucleic acids with high affinity at or close to room temperature, and providing excellent mismatch discrimination will be valuable for generating an essentially complete library of genotyping probes, applicable for typing majority of SNPs. Affinity of DNA probes and all other nucleic acid probes available so far, including peptide nucleic acids (PNAs), is insufficient to allow generating libraries of short probes fulfilling these criteria.[24] To date, PNA probes had to be at least seven-nucleobase long because the lower affinity of shorter probes made their hybridization at room temperature unfavorable.[24] Moreover, locked nucleic acid (LNA) molecules form exceedingly stable duplexes with complementary target nucleic acids.[25, 26] However, the probes used to test hybridization of very short LNAs are dye-labeled and, therefore, their synthesis is

prohibitively expensive and labor-demanding.[24, 27] Short LNAs have been applied for efficient SNP scoring using fluorescence polarization detection.[24] There was an attempt to decrease length of SNP probes by using LNA hexamers, which required only 4096 oligonucleotides in the complete library.[28, 29] However, these hexamers exhibit several shortcomings[29] including difficulties in discriminating terminal mismatches.

As a proof of concept, we herein designed and synthesized a new 2,2'-bithien-5-yl polymeric nucleic acid analog for SNP typing. We explored a model example of the electrochemically synthesized 2,2'-bithien-5-yl TTTATA hexamer selectively hybridizing genetically important AT-rich ODN via Watson-Crick nucleobase pairing[1] with perfect discrimination of one nucleobase mismatch. The resulting 2,2'-bithien-5-yl hexamer was designed to assume a predefined structure by taking advantage of sequence programmability of the DNA template. Herein, we used the ODN template to dictate precise positioning of 2,2'-bithien-5-yl functional monomers around the A and T rich template. Using molecular imprinting, we approached effortlessly the manner, at which nature generates complexity and function.[8] Moreover, we used two templates, namely, an ODN of the TATAAA **1** (Scheme 1) and structurally similar PNA **2** (Scheme 1) of the same sequence as that of TATAAA. In eukaryotes, the TATAAA is a part of the DNA core promoter, which is critical for proper regulation of the gene-selective transcription.[30] For effective AT-rich oligonucleotide-template imprinting, we designed and synthesized electropolymerizable bis(2,2'-bithien-5-yl)methane functional monomers with T or A nucleobase moiety, vis., 4-bis(2,2'-bithien-5-yl)methylphenyl 2-adenine ethyl ether[31] **3** (Scheme 1) and 4-bis(2,2'-bithien-5-yl)methylphenyl thymine-1-acetate **4** (Scheme 1). The 2,2'-bithien-5-yl moiety of **3** and **4** is capable of electropolymerization resulting in a stable conducting polymer.[32] Moreover, nucleobase-substituents of the 2,2'-

bithien-5-yl functional monomers recognized compatible nucleobases of the oligonucleotide-template used to form a pre-polymerization complex. In this complex, **3** and **4** were self-assembled around template molecules via Watson-Crick nucleobase pairing. Subsequently, this complex was structurally incurred with the 2,4,5,2',4',5'-hexa(thiophene-2-yl)-3,3'-bithiophene **5** (Scheme 1)[33] cross-linking monomer by electropolymerization. DNA-directed electropolymerization of functional monomers resulted in the 2,2'-bithien-5-yl TTTATA hexamer complementary to the TATAAA in the resulting molecularly imprinted polymer (MIP). In this MIP, the artificial TTTATA probe hybridized the native TATAAA to form a double-stranded hybrid as an artificial TATAAA promoter sequence.

The aim of the present research was to identify molecular changes in genetically relevant ONs using the most innovative methods of molecular analysis. By connecting these methods with MIPs, we developed a procedure of preparation of simple, rapidly operating, and inexpensive chemosensors. These chemosensors were sensitive and selective for direct, non-labeled ON determination using 2,2'-bithien-5-yl MIP, whose thickness was controlled by the amount of charge passed during the deposition. Notably, conducting polymer films prepared by electropolymerization grow directly at a precise location on the transducer surface. Therefore, these polymers have increasingly been used for preparation of MIP films as chemosensor recognizing units.[32, 34, 35] Further development of the proposed molecular imprinting procedure may lead to generation of a set of genotyping electrosynthesized 2,2'-bithien-5-yl hexamer probes, constructing for instance electrode arrays with multiplexed electrochemical detection systems.

To date, different DNA sensors have been devised[36] and the number of those using MIP films as recognition units is steadily growing.[37, 38] Different imprinting methods were developed

for recognition and determination of nucleic acid targets ranging from small nucleobases[31, 39, 40] to single- (ssDNA)[41] and double-stranded (dsDNA)[42] long-chain DNAs. However, the possibility of preparation of an MIP engaging programmability of the ODN template for controlling sequence of the oligomer prepared via electropolymerization of nucleobase-substituted functional monomers, including molecular imprinting of non-labeled ONs using Watson-Crick nucleobase pairing,[1] has not been explored yet.

2. Material and Procedures

The **Reagents and chemicals** as well as **Instrumentation and procedures** sections are provided in Supporting Information.

2.1 Preparation of MIP films, and then template extraction from these films

First, two solutions of pre-polymerization complexes with different templates were prepared. For that, functional and cross-linking monomers were dissolved in acetonitrile or a mixture of acetonitrile, toluene, water, and isopropanol with either the PNA or DNA template. Then, MIP films were prepared by potentiodynamic electropolymerization with the potential scanned from 0.50 to 1.25 V and back at the rate of 50 mV/s. After electropolymerization, the MIP film was rinsed with abundant acetonitrile to remove unbound pre-polymerization complex components and the supporting electrolyte. Subsequently, the TATAAA or the PNA template was extracted from the film with 20% trifluoroacetic acid or 0.1 M NaOH, respectively, for 45 min at room temperature in order to vacate imprinted cavities in the MIP before recognizing the TATAAA analyte.

In the same manner, a chemosensor featuring a control non-imprinted polymer (NIP) film was prepared, however, in the absence of the template in the solution for electropolymerization.

3. Results

3.1 Confirmation of formation of stable A-T Watson-Crick nucleobase pairs in the pre-polymerization complex

Formation of stable A-T nucleobase pairs in the pre-polymerization complex was predicted by computational modeling and experimentally confirmed by the isothermal titration calorimetry (ITC) measurements, described below.

For favorable formation of a pre-polymerization complex in solution, initial self-assembly of the template and functional monomers is crucial.[43] Structural modeling is helpful for that. However, an accurate ab initio optimization of the 568-atom complex of one TATAAA template molecule with two adenine **3** and four thymine **4** functional monomer molecules appeared to be prohibitively time consuming in our case, even with the RI approximation[44] adopted. Therefore, we focused on the complexation of a shorter TATA fragment with functional monomers **3** and **4**, and then performed molecular modeling at the B3LYP level with the 3-21G(*) basis set (Scheme S1). The negative Gibbs energy gain as high as ΔG = -256.6 kJ/mol was calculated using the density functional theory (DFT) method augmented with the D3 empirical dispersion correction.[45-48] Although this value, calculated per one hydrogen bond, is higher than that for typical nucleobase pairing interactions, our results still seem to be qualitatively correct and should not change significantly even at a higher level of the theory. This relatively high negative ΔG value clearly indicates an energetic preference of formation of a complex of TATA with the A and T moieties of the functional monomers, each paired with the complementary T and A moiety, respectively, of the TATA. Apparently, the 5'-TATAAA-3' recognition mimicked that of nucleic acids in living organisms.

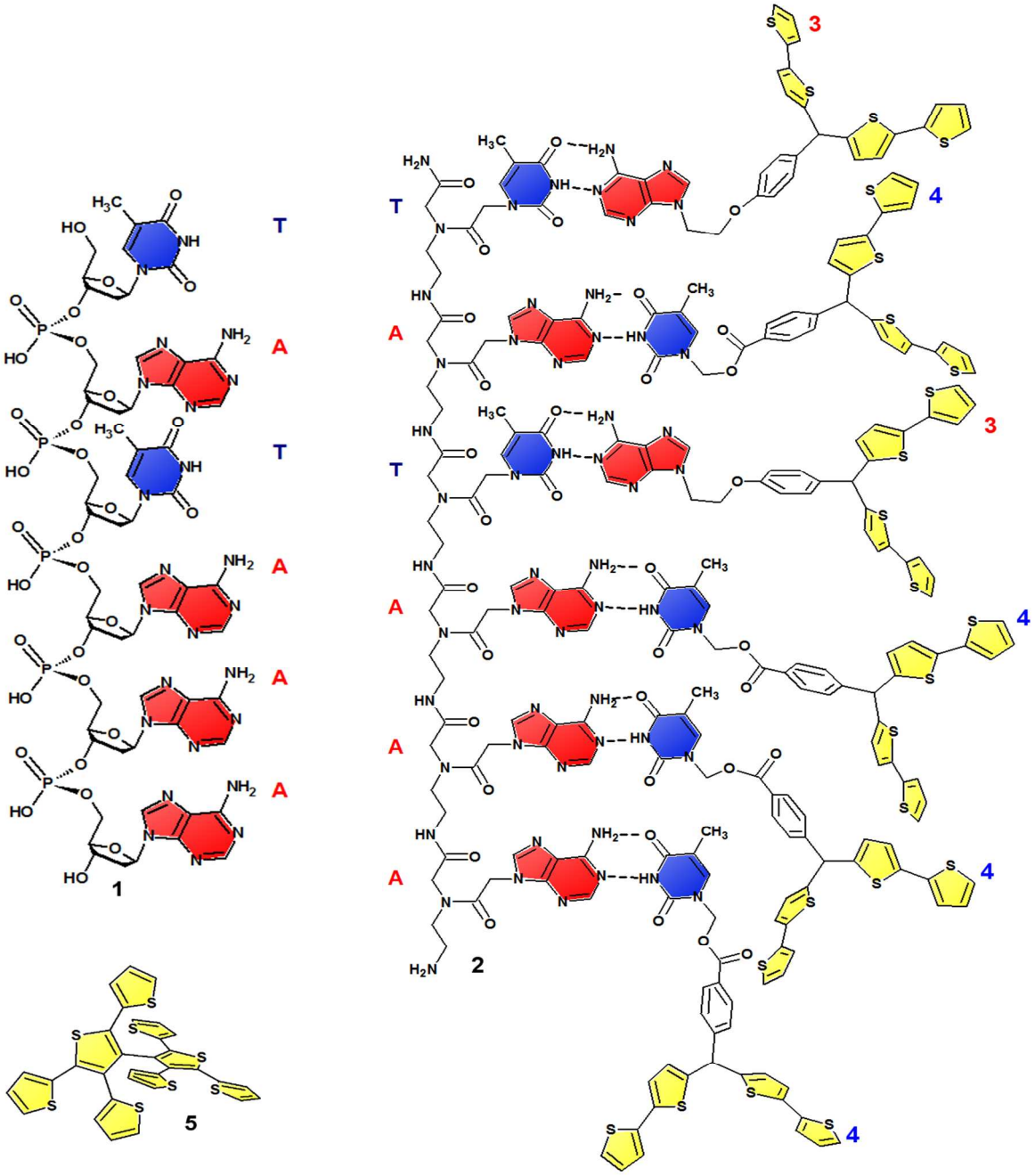

Scheme 1. Structural formulas of the TATAAA oligonucleotide **1**, its PNA analog with the same nucleobase sequence **2**, 4–(bis(2,2'–bithien–5–yl)methylphenyl-2-adenine ethyl ether **3** and 4-(bis-2,2'-bithien-5-yl)methylphenyl thymine-1-acetate **4** functional monomers as well as the 2,4,5,2',4',5'-hexa(thiophene-2-yl)-3,3'-bithiophene **5** cross-linking monomer.

For experimental confirmation of formation of the A-T nucleobase pairs between the recognizing moieties of functional monomers and the binding nucleobase moieties of the

template in solution, we performed an ITC measurement (Fig. S1). However, solubility of the functional monomers and DNA or PNA in the solution for electropolymerization was insufficient to reach the concentrations required for the titration. Therefore, instead, we used DMSO as the solvent because it dissolved both **2** and **3**. Moreover, stability of PNA, in contrast to stability of DNA, is almost unaffected by organic solvents.[49] The total calorimetric enthalpy change was obtained by subtracting the dilution heat of titrant **3** from the total heat corresponding to injections of the solution of this titrant to the solution of the PNA template. An independent model was chosen and a theoretical isotherm was fitted to the ITC data acquired yielding the binding enthalpy change (ΔH = -19.0 kJ), the complex stability constant ($K_s = 1.65\times10^5$ M^{-1}), and the expected complex stoichiometry (**3** : PNA = 1 : 2). From these values, the change of Gibbs energy (ΔG = -29.5 kJ/mol) and entropy (ΔS = 35.7 J mol^{-1} K^{-1}) of complex formation were calculated. Apparently, the complex of one PNA template molecule and two adenine functional monomer molecules was stable.

3.2 Deposition of MIP films on different electrodes

Figure 1 presents successful electropolymerization of the PNA-(**3** and **4**) complex to form a PNA imprinted MIP film. The anodic peak at ~1.17 V vs. Ag/AgCl in the first current-potential cycle (Fig. 1a) corresponds to electro-oxidation of the (2,2'-bithien-5-yl)methane moieties of functional monomers **3** and **4** as well as of cross-linking monomer **5**. In the subsequent cycle, current increased indicating deposition of an electroactive polymer film. Thus, this film did not hinder the charge transfer needed for further electro-oxidation of the monomers. Simultaneously, resonance frequency decreased as a result of the QCR mass increase after the MIP-PNA film deposition. Additionally, simultaneous negligible decrease (2 Ω) of the dynamic resistance in the first cycle, and then its return to the background line in the second cycle (not

shown), indicated that the MIP-PNA film was rigid. Then, the film was imaged by atomic force microscopy, AFM (inset to Figure 1), in order to unravel its morphology and thickness. Apparently, this film was composed of well-defined grains with diameter in the range of 30 to 60 nm. Its thickness was 114(±5) nm, as determined from the height of the step formed after removing part of the film from the substrate surface with a Teflon spatula.

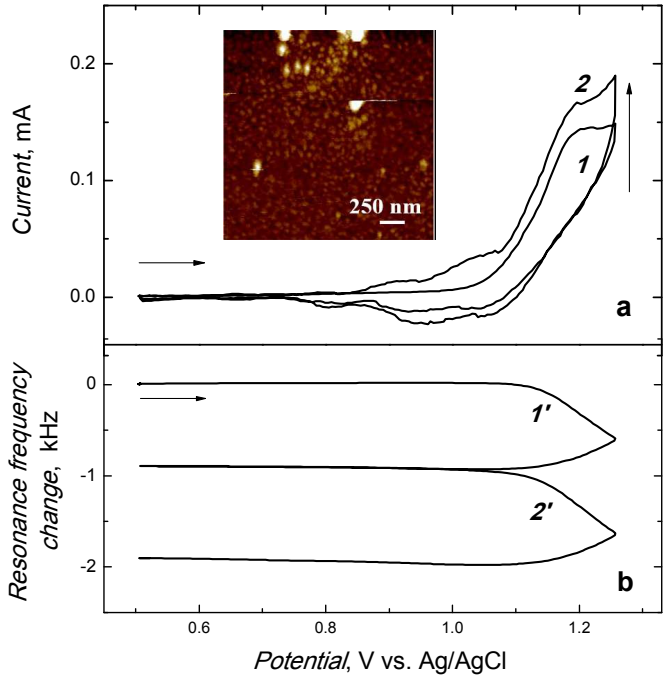

Figure 1. Simultaneously recorded two-cycle curves of (a) current and (b) resonance frequency change vs. potential for deposition on the Au-quartz electrode of the PNA-templated MIP film by potentiodynamic electropolymerization from the 40 μM PNA, 0.1 mM adenine functional monomer **3**, 0.2 mM thymine functional monomer **4**, and 0.2 mM cross-linking monomer **5**, 0.1 M (TBA)ClO_4 solution of acetonitrile. The potential scan rate was 50 mV s^{-1}. Cycle numbers are indicated at curves. Inset represents atomic force microscopy (AFM) image recorded using the tapping mode for the PNA-imprinted polymer. Image size is (2 × 2) mm^2.

We applied this MIP-PNA film as the recognition unit of a chemosensor for selective determination of the TATAAA analyte. For that, the PNA template was extracted with 20% trifluoroacetic acid. The increase of the resonance frequency after extraction evidenced the MIP-PNA mass decrease because of PNA removal (Fig. S2). Thus, the emptied MIP-PNA cavities

featuring 2,2'-bithien-5-yl TTTATA recognizing sites could be used to recognize the AT-rich TATAAA analyte. Herein, we demonstrated MIP film binding of the PNA under FIA conditions (Fig. S3) and, moreover, the TATAAA (not shown). The comparable resonance frequency drop indicated equal affinity of the MIP to both the TATAAA and its PNA close analog manifested by hybridization via Watson-Crick pairing. As expected, this was possible because the spacing between the nucleotides in TATAAA is the same as that in PNA.[50]

3.3 Characterization of TATAAA-imprinted MIPs

We extensively characterized the TATAAA-templated MIP film to examine if the sequence-defined stable 2,2'-bithien-5-yl TTTATA oligomer, structurally not related to nucleic acids, reveals properties of conducting 2,2'-bithien-5-yl oligomers and exhibits spectral and chemical properties of DNA analogs. Herein, the 2,2'-bithien-5-yl TTTATA was characterized by polarization-modulated infrared reflection-adsorption spectroscopy (PM-IRRAS) (Fig. 2a) and X-ray photoelectron spectroscopy, XPS (Table S1). Moreover, its hybridization was confirmed by the differential pulse voltammetry, DPV (Fig. 2b), electrochemical impedance spectroscopy, EIS (Fig. S4), piezoelectric microgravimetry, PM (Fig. 3), surface plasmon resonance, SPR (Fig. S5a and b), and capacitive impedimetry, CI (Fig. 4) measurements.

3.3.1 PM-IRRAS characterization of the MIP film

We carried out PM-IRRAS measurements in search for spectral properties typical of polybithiophenes and DNA analogs in the 2,2'-bithien-5-yl TTTATA oligomer (Fig. 2a). The presence of bonds in regions of 1580–1320 cm^{-1} and 1290–1140 cm^{-1}, characteristic of vibrations of polybithiophene bonds, confirmed the presence of the 2,2'-bithien-5-yl backbone of the resulting DNA analog. Moreover, there was a broad set of bands in these regions characteristic

of vibrations of nucleobase bonds. Thus, DNA hybridization was confirmed. However, relative intensity of these peaks was higher when the 2,2'-bithien-5-yl TTTATA oligomer hybridized with the TATAAA analyte in the MIP matrix (spectrum *1* in Fig. 2a). Then, intensities of these bands decreased after extraction of the TATAAA template (spectrum *2* in Fig. 2a), thus resulting in the dehybridized 2,2'-bithien-5-yl TTTATA oligomer in MIP cavities. Moreover, nucleobase pairing of the template with functional monomers was proved by enhancement of the band at 1690 cm^{-1} corresponding to C=O stretching vibration (spectrum *1* in Fig. 2a). After extraction, this band disappeared (spectrum *2* in Fig. 2a) as a result of dehybridization.[51]

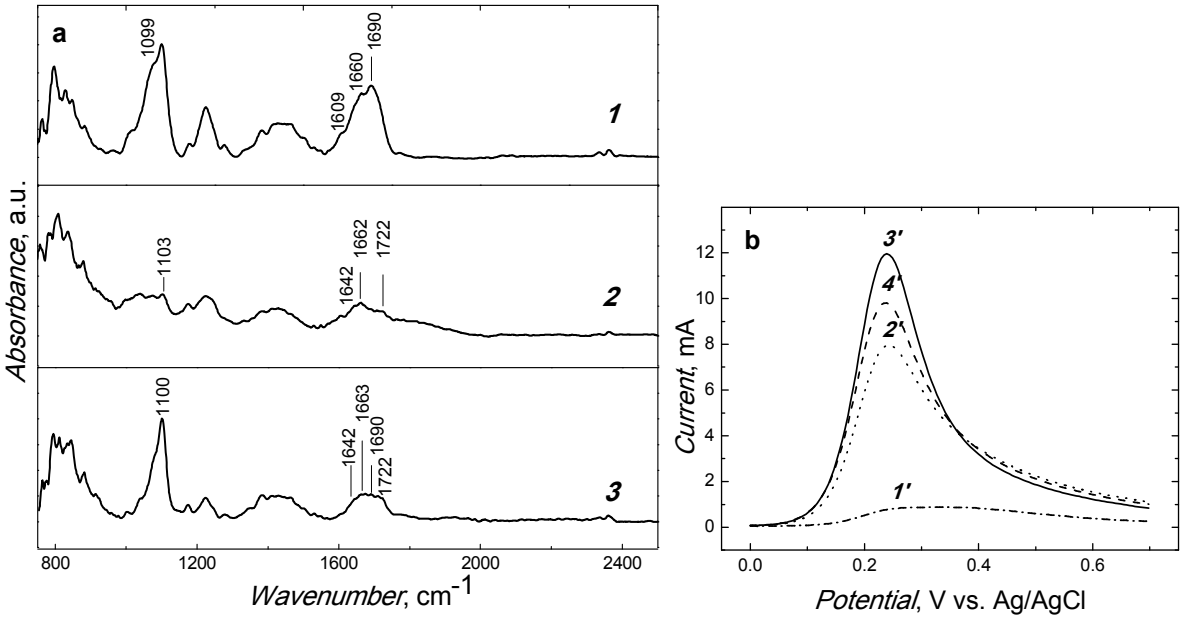

Figure 2. (a) The normalized PM-IRRAS spectra of the MIP-TATAAA film (*1*) before and (*2*) after TATAAA extraction with 0.05 mM NaOH as well as (*3*) the non-imprinted polymer film. All films were deposited on Au-glass slides. (b) Differential pulse voltammograms for 0.1 M $K_4Fe(CN)_6$ in 0.1 M KNO_3, recorded at the 1-mm diameter Pt disk electrode coated with the MIP film (*1'*) before and after (*2'*) 25, and (*3'*) 45 min of TATAAA extraction with 0.1 M NaOH, and then (*4'*) after immersing the electrode in 50 μM TATAAA for 15 min. The film was prepared by potentiodynamic electropolymerization in the potential range of 0.50 to 1.25 V vs. Ag/AgCl at the 50 mV s^{-1} scan rate.

However, there were still bands characteristic of bending vibrations of the free -NH_2 group of A as well as stretching vibrations of C=O groups at C2 and C4 of T, located at 1642, 1662, and 1772 cm^{-1}, respectively. By comparing bands of this region with those of the NIP spectrum (spectrum *3* in Fig. 2a), we concluded that neither the A nor T substituent of 2,2'-bithien-5-yl functional monomer **3** and **4** is paired in the NIP film.

In the spectrum of the NIP film (spectrum *3* in Fig. 2a), there are bands characteristic of the -NH_2 group of the unpaired adenine moiety and the C=O group of the unpaired T moiety at 1642 and 1663 cm^{-1}, respectively, although of low intensity. These wavenumbers values indicate no A-T base pairing between functional monomers themselves. Moreover, low intensity of the band at 1690 cm^{-1} characteristic of hybridization indicates no mutual pairing of the A and T functional monomers between themselves.

The band at ~1100 cm^{-1} is characteristic of the (TBA)ClO_4 supporting electrolyte salt[52] (spectra *1* and *3* in Fig. 2a). As expected, it nearly disappeared after template extraction (spectrum *2* in Fig. 2a).

3.3.2 Electrochemical characterization of the MIP film

In the DPV using "gate effect" studies of the MIP film with the TATAAA template molecules occupying the imprinted cavities, current peak of the $Fe(CN)_6^{4-}$ oxidation (curve *1* in Fig. 2b) was hardly seen. Moreover, in EIS studies the Nyquist plot for the Pt disk electrode, coated with the TATAAA-templated MIP film, was represented by a large arc related to high charge transfer resistance, R_{ct} = 13 kΩ (curve *1* in Fig. S4), of the $Fe(CN)_6^{4-}/Fe(CN)_6^{3-}$ redox probe. Apparently, the TATAAA template presence in the MIP film hindered the $Fe(CN)_6^{4-}/Fe(CN)_6^{3-}$ electrode process. Next, the template was gradually removed from imprinted cavities (Fig. 2b), thus allowing for probe free permeation through the MIP film, as confirmed by the DPV peak

increase in the consecutive steps of extraction (curves *2* and *3* in Fig. 2b). Furthermore, diameter of the arc part of the Nyquist plot smaller than that in curve *1* in Figure S4, implied a lower charge transfer resistance (R_{ct} = 2.04 kΩ) of the template-free MIP film coated electrode. After complete template extraction, the resulted 2,2'-bithien-5-yl TTTATA immobilized in molecular cavities of the MIP film hybridized the TATAAA analyte. In effect, the DPV peak decreased after immersing this electrode in the TATAAA analyte solution, thus confirming that redox probe diffusion in the film was hindered again. Moreover, diameter of the resulting arc of the Nyquist plot increased to R_{ct} = 2.42 kΩ, thus indicating that the target TATAAA analyte was bound by the TTTATA site in the MIP film (curve *3* in Fig. S4).

3.3.2 Analytical performance of the MIP chemosensor for TATAAA determination using capacitive impedimetry (CI), piezoelectric microgravimetry (PM), and surface plasmon resonance (SPR) spectroscopy

We examined analytical performance of the TATAAA-extracted MIP chemosensor with respect to TATAAA determination by using PM and CI, both under FIA conditions, as well as SPR spectroscopy under stagnant-solution conditions (Table 1). Moreover, we investigated the kinetic aspect of the TATAAA recognition with the 2,2'-bithien-5-yl TTTATA oligomer using both the PM and SPR spectroscopy transduction (see below, in Discussion).

Analytical parameters of our chemosensors with respect to TATAAA determination are summarized in Table 1.

Table 1. Analytical parameters of MIP chemosensors for TATAAA determined with different techniques.

TATAAA chemosensor	Limit of detection (LOD), nM	Sensitivity, x, y, or z	Dynamic linear concentration range, μM
Capacitive impedimetry (CI)[a]	5	2.07(±0.13)[x]	0.05-2.00
Surface plasmon resonance (SPR) spectroscopy[b]	50	3.43(±0.30)[z]	0.05-7.50
Piezomicrogravimetry (PM)[a]	110	1.07(±0.04)[y]	0.5-100

[a] under FIA conditions
[b] under stagnant-solution conditions with neither gold NPs nor protein enhancement
[x] μF cm^{-2} μM^{-1}
[y] Hz μM^{-1}
[z] RU μM^{-1}

3.3.2.1 Piezoelectric microgravimetry (PM) chemosensor

We determined the TATAAA analyte hybridized in molecular cavities of MIP using PM-FIA. After each injection, resonance frequency decreased (Fig. 3a) because the analyte entered the film and, accordingly, the film mass increased, as Sauerbrey equation predicts. After reaching minimum, this frequency increased to its initial baseline value indicating a complete removal of the analyte from the film by excess of the carrier solution. Figure 3a shows resonance frequency change with time for six consecutive injections of the TATAAA analyte solutions of different concentrations, which allowed constructing calibration plots (Fig. 3b).

The chemosensor response to the TATAAA analyte was linear in the concentration range of at least 0.5 to 10 μM. It was described by the linear regression equation of Δf [Hz] = -0.66(±0.02) [Hz] -1.07(±0.04) [Hz μM^{-1}] c_{TATAAA} [μM]. The LOD, sensitivity, and correlation coefficient at $S/N = 3$ was 110 nM, 1.07(±0.04) Hz μM^{-1}, and 0.99, respectively. The sensitivity of the NIP control film to the TATAAA was four times lower equaling 0.27(±0.03)

Hz μM^{-1} and, therefore, a reasonably high imprinting factor of 4.0 was calculated from the ratio of the sensitivity of the MIP and NIP film to TATAAA.

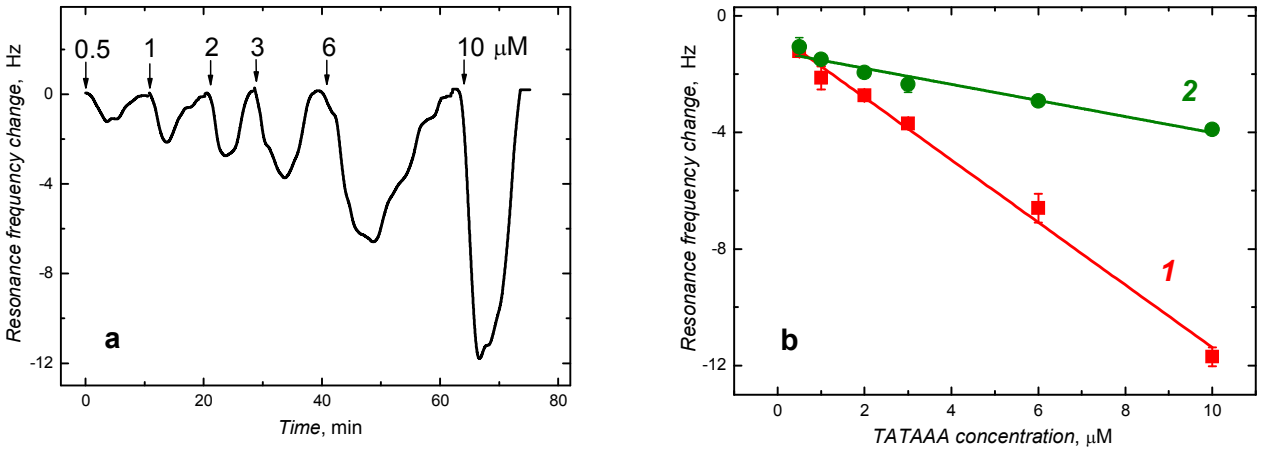

Figure 3. (a) The resonance frequency change with time for repetitive FIA injections of TATAAA of the concentration indicated at each peak for the MIP-TATAAA film coated Au-QCR. (b) Calibration plots for TATAAA on the (*1*) TATAAA-extracted MIP and (*2*) NIP film. The flow rate of the PBS (pH = 7.4) carrier solution was 30 μL/min.

3.3.2.2 Surface plasmon resonance (SPR) spectroscopy chemosensor

In SPR spectroscopy measurements under stagnant-solution conditions, binding the TATAAA analyte to the recognizing complementary TTTATA probe induced a change in the film refractive index. This change was proportional to the mass load of the film, thus enabling real-time hybridization monitoring. Herein, the TATAAA analyte caused a shift of the reflectivity to higher angles as a result of significant change in the refractive index of the SPR chip coated with the MIP film (Fig. S5a).

The SPR calibration plot constructed for the TATAAA analyte (Fig. S5b) was described by the linear regression equation of ΔR [RU] = 8.22(±0.49) [RU] + 3.43(±0.30) [RU μM^{-1}] c_{TATAAA} [μM] where *R* stands for the refractive index. The LOD reached was appreciably low equaling ~50 nM TATAAA, which is half that attained herein by PM. This is particularly

important because we enhanced the response of the SPR chip with neither gold nanoparticles nor proteins.

3.3.2.3 Capacitive impedimetry (CI) chemosensor

In CI determination of TATAAA under FIA conditions, we evaluated the electrical double-layer capacity, C_{dl}, at the Pt-MIP interface by measuring the imaginary component of impedance, Z_{im}. Considering only the compact part of the double layer, we used Equation 1 for C_{dl} determination at the Pt-MIP interface by measuring Z_{im},

$$Z_{\mathrm{im}} = \frac{1}{\omega C_{\mathrm{dl}} A} \quad (1)$$

where $\omega = 2\pi f$ and A stands for angular frequency and Pt electrode surface area, respectively.

The determined C_{dl} changes corresponded to changes of capacity of the compact part of the double layer solely depending on the changes of electric permittivity, ε, and the double-layer thickness, d, according to Equation 2

$$C_{\mathrm{dl}} = \frac{\varepsilon \varepsilon_0 A}{d} \quad (2)$$

where ε_0 is permittivity of free space. After TATAAA binding, the permittivity increased, so did the capacity. Apparently, the recognizing MIP film reversibly bound the analyte.

Based on the CI measurements, we constructed calibration plots for the MIP and NIP film coated electrodes (curves *1 – 3*, and *4*, respectively, in Fig. 4b). The linear dynamic concentration range extended from at least 0.05 to 2.0 μM TATAAA (curve *1* in Fig. 4b) obeying the linear regression equation of C_{dl} [μF cm^{-2}] = 2.67(±0.13) [μF cm^{-2}] + 2.07(±0.13) [μF cm^{-2} μM^{-1}] c_{TATAAA} [μM]. The LOD, determined at $S/N = 3$, reached as low value as ~5 nM

TATAAA. The sensitivity and correlation coefficient was 2.07(±0.13) μF cm^{-2} μM^{-1} and 0.98, respectively.

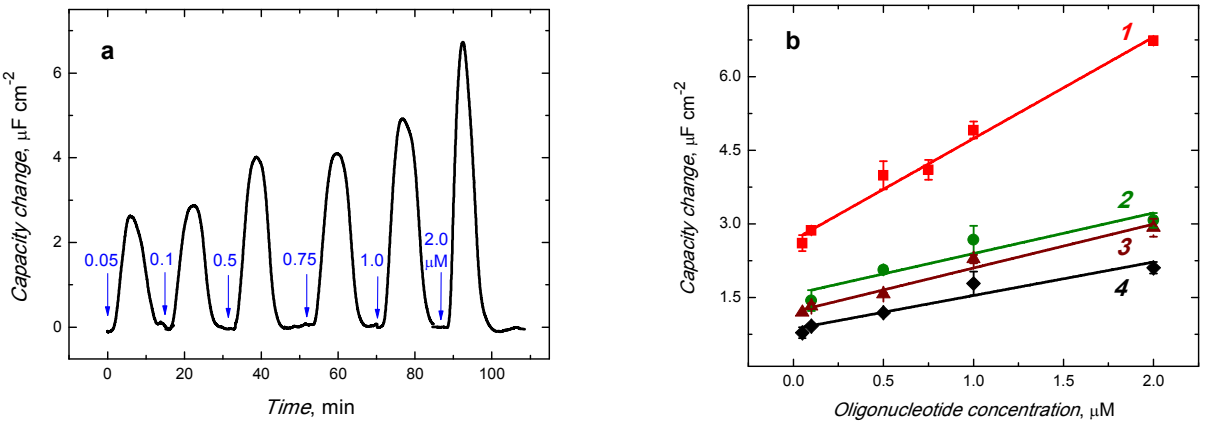

Figure 4. (a) The capacity change with time in response to repetitive FIA 200-μL injections of 0.1 M NaF solutions of TATAAA for MIP film coated Pt disk electrode. The TATAAA concentration is indicated at each peak. The flow rate of 0.1 M NaF, serving as the carrier solution, was 20 μL/min. (b) Calibration plots for (*1*) TATAAA, (*2*) TATAGA, (*3*) TATAAG, on the TATAAA-extracted MIP film deposited on the Pt disk electrode, and (*4*) TATAAA on the NIP film deposited on the Pt disk electrode.

The chemosensor selectivity was determined under the same CI conditions of FIA by examining sensitivity of the MIP film to interfering oligonucleotides of the sequence similar to that of the TATAAA analyte including TATAAG and TATAGA, i.e., hexamers mismatched with just one nucleobase. The MIP chemosensor was ~3.0 and ~2.3 times more sensitive to the TATAAA analyte than to the TATAGA and TATAAG interference, respectively. Moreover, TATAAA was determined at a control NIP film (curve *4* in Fig. 2b), to confirm the imprinting. Apparently, the TATAAA binding by the NIP was significantly (~2.5 times) weaker compared to that of the MIP revealing sensitivity of 0.82(±0.19) μF μM^{-1}.

4. Discussion

The MIP formation in organic solvent solutions is more effective than that in aqueous solutions, if non-covalent binding is involved in molecular imprinting.[53] To date, most of MIP syntheses involving non-covalent template binding were performed using organic solvents in order to avoid water competition in hydrogen bonding operative in formation of the pre-polymerization complex. Moreover, contribution of hydrogen bonding is higher, the lower is electric permittivity of the solvent used. Therefore, derivatives of all five nucleobases soluble in an organic solvent were used as templates.[54] Among them, MIPs prepared using genuine nucleobases are most desired since the ultimate objective of this imprinting is recognition of native components of nucleic acids. Unfortunately, most of these components of biological origin are insoluble in organic solvents. Therefore, functional monomers soluble in aqueous solutions addressed this need.[41, 42, 55]

Herein, we designed and fabricated functional monomers soluble in aprotic solvents and capable of recognizing nucleobases of nucleic acids via Watson-Crick pairing. Functional monomers synthesized herein formed a non-covalent complex with the ON template. Then, this complex was electropolymerized to form 2,2'-bithien-5-yl conducting oligomers co-joined to this ON. Moreover, the present ON template imprinting, which restricted the Watson-Crick nucleobase pairing between its nucleobases and nucleobases of functional monomers aligned along the AT-rich oligonucleotide, resulted in the nucleobase-substituted 2,2'-bithien-5-yl hexamer probe selectively hybridizing the matched ON. Thus, molecular imprinting provided means to utilize the sequence programmability of DNA to prepare any number of stable 2,2'-bithien-5-yl oligomers designed to reveal properties of a stable DNA analog fabricated in molecular cavities of the MIP.

We anticipated that the use of the PNA analog of DNA, soluble in aprotic solvents, can appreciably increase efficiency of molecular imprinting using our 2,2'-bithien-5-yl functional monomers. However, PNA has to be pre-organized to assume binding conformation before complexation for successful use of the imprinting strategy, i.e., to ensure high affinity and selectivity of binding the functional monomers and the PNA template. Unlike DNA or RNA in the non-hybridized (single-stranded) form, which can adopt a helical structure through base-stacking (although highly flexible), PNA does not exhibit well-defined conformational folding in solution.[56] This is because PNA is a neutral DNA analog where the negatively charged phosphodiester backbone of DNA (Scheme 1) is replaced with an achiral 2-amino-ethyl-glycine (AEG).[57] Moreover, PNA oligomers form very stable duplexes with complementary target nucleic acids via Watson-Crick nucleobase pairing. We confirmed this pairing between PNA and our nucleobase-substituted 2,2'-bithien-5-yl functional monomers. Apparently, functional monomers enforced conformational stability of the PNA template and provided the size and hydrogen bonding complementarity for effective PNA imprinting. Therefore, the pre-polymerization complex of PNA with complementarily aligned 2,2'-bithien-5-yl functional monomers **3** and **4** was very stable. This stability was confirmed by a relatively high melting temperature (T_m = 63.9 °C) of the pre-polymerization complex determined with the differential scanning calorimetry (DSC) measurement (Fig. S6). Moreover, this T_m is higher than that of a comparable ON, which ranges from 10 to 43 °C for TATTTTA and ATGGTG, respectively.[24] Herein, **3** or **4** functional monomers, used as artificial nucleotides, carry the sequence information of DNA at the molecular level. Therefore, we propose the use of stable, nucleobase-substituted 2,2'-bithien-5-yl oligomers as non-biological oligonucleotide

counterparts. Apparently, our results open up possibilities to store and retrieve digital data using DNA molecules.

First, our PM-FIA measurements confirmed that emptied molecular cavities in the MIP-PNA successfully recognized by hybridization both PNA and TATAAA with similar affinity. Next, we examined if a minute amount of water, needed to dissolve the TATAAA and to maintain its native conformation during imprinting, influenced recognition properties of the MIP film of the chemosensor. Moreover, we have demonstrated that a minute amount of a protic solvent can be added to the pre-polymerization complex solution to prepare the MIP recognizing TATAAA with the same affinity as that of the PNA-imprinted MIP prepared using just one aprotic solvent. Therefore, the MIP film bound the TATAAA analyte with the same affinity as that of the MIP-PNA film (not shown).

Thus, we developed two procedures of imprinting AT-rich ON, using nucleobase-substituted 2,2'-bithien-5-yl functional monomers designed for the Watson-Crick pairing. We prepared MIP chemosensors considering their recognition of secondary structure of the determined AT-rich ON analyte. We have demonstrated that this determination was possible because we fabricated, inside MIPs, artificial non-labeled hexameric probes with a very high affinity for complementary nucleic acid targets, both DNA and PNA. Our constrained 2,2'-bithien-5-yl DNA analog hybridized the TATAAA at room temperature under FIA conditions within 2 min. Moreover, its sensitivity for mismatch discrimination makes it uniquely suited for hybridization-based SNP genotyping.

Herein, we exploited the complementary information about the TATAAA-templated MIP film provided by the XPS multipoint surface analysis [58, 59] to identify surface elemental composition of the film and spatial atomic distribution (Table S1). Apparently, the MIP film

with 2,2'-bithien-5-yl TTTATA was homogeneous. That is, 3-D molecular cavities were homogeneously imprinted in it and nucleobases of the electrochemically synthesized 2,2'-bithien-5-yl TTTATA oligomer were available for Watson-Crick pairing of nucleobases of the TATAAA. The TATAAA is the only source of phosphorus in the studied system. Therefore, its presence, evidenced by XPS, confirmed the TATAAA imprinting to form the TTTATA-TATAAA hybrid in the MIP film, on the one hand. On the other, however, its subsequent absence in the film after extraction (not shown) confirmed complete template removal from MIP.

Kinetic analysis of the PM-FIA data of the TATAAA analyte interaction with the MIP[60, 61] provided values of the association, $k_a \approx 10^4$ M^{-1} s^{-1}, and dissociation, $k_d = 10^{-2}$ s^{-1}, rate constants. From this analysis, we concluded that the TTTATA hexamer hybridized TATAAA with a high value of the complex stability constant, $K_s^{\text{TTTATA-TATAAA}} = k_a/k_d \approx 10^6$ M^{-1}, comparable to that characteristic for longer-chain DNA-PNA hybrids. We determined the above rate constants by fitting theoretical data to experimental PM-FIA data. These constants well compared with those determined from the SPR analysis using the literature procedure.[60, 61] To date, a state-of-art SPR biosensor detected a short (15-mer) oligonucleotide target ($M_w = 5$ kDa) via complementary probe hybridization with a similar k_a value of 10^4 $M^{-1}s^{-1}$.[62] Moreover, stability constants of complexes of native nucleic acid "hosts" with their cognate ligand "guests" are relatively low being of the order of 10^3 M^{-1}.[63] Successfully, the presently determined $K_s^{\text{TTTATA-TATAAA}}$ value for the hexamer probe is comparable to those for much longer-chain DNA-PNA hybrids, 10^6 M^{-1} (for PNA-GCAT**TT**GCAT) $\leq K_s^{\text{DNA-PNA}} \leq 10^7$ M^{-1} (for PNA-GCAT**GA**GCAT).[64, 65] Our procedure circumvents disadvantages connected with a very low stability of short ON hybrids.

With the presently developed procedure, we fabricated an oligomer analog of DNA in the molecular cavities of MIPs. Herein, we assumed that our MIP film prevented nonspecific adsorption and aggregation of 2,2'-bithien-5-yl nucleic acid analogs on the transducer surface, which is critically important for surface hybridization assays.[66-68] Furthermore, this film most likely operated as a shield for the 2,2'-bithien-5-yl TTTATA located in its imprinted cavities, thus protecting degradation of this hexamer strand from nuclease. Presumably, even without a distinct stage of our hexamer SNP probe immobilization, its 2,2'-bithien-5-yl backbone was aligned in parallel to the transducer surface. Therefore, effects of counterion screening[68] were minimized. The probe horizontally immobilized on the surface is important for DNA hybridization assays that use the electric field effect sensors for detection. This alignment does not limit the probe length, as is the case with the conventional vertically tethered probe.[68] Moreover, our 2,2'-bithien-5-yl MIPs are invulnerable to inhibition by sample components[69, 70] that can result in false negative determinations in clinical,[71, 72] environmental,[73] food,[74] and forensic[75] samples. Therefore, our direct method of quantification of specific sequences is a promising alternative to quantitative amplification methods, such as PCR reliant on polymerases.[76, 77]

5. Conclusions

By combining of PM, SPR, or CI signal transduction with the MIP film recognition, we have successfully developed a procedure of simple, inexpensive, rapid, and label-free chemosensing of the TATAAA analyte by using the 2,2'-bithien-5-yl TTTATA probe. Under carefully chosen FIA conditions, i.e., at a relatively low flow rate of the carrier solution and a large volume of the injected sample solution, the concentration limit of detection was as low as ~5 nM TATAAA. The developed strategy of MIP preparation enables utilization of the self-recognizing properties

and sequence programmability of DNA to generate tailored artificial oligomers. Thus, the present proof-of-concept study opens up new horizons in designing conducting 2,2'-bithien-5-yl DNA analogs with discrimination of one nucleobase mismatch in the determined oligonucleotide at room temperature within 2 min. Further development of the proposed procedure may lead to a new generation of DNA chemosensors for determination of self-complementary sequences (e.g., inverse repeats, palindromes, or hairpins), regardless of their sequence. Such a work is in progress in our laboratories.

ASSOCIATED CONTENT

Supporting Information

Optimized structure of the TATA complex, experimental data of ITC, EIS, SPR, and DSC measurements, PM characteristic of the PNA-MIP film

AUTHOR INFORMATION

Corresponding Author

*E-mail addresses: apietrzyk@ichf.edu.pl; wkutner@ichf.edu.pl; francis.dsouza@unt.edu

Author Contributions

The manuscript was written through contributions of all authors. All authors have given approval to the final version of the manuscript.

ACKNOWLEDGMENT

We thank Dr. Tiziana Benincori (Department of Chemical and Environmental Sciences, University of Insubria, Como, Italy) for synthesizing the cross-linking monomer **5**, Dr. J. Jemielity, Ph.D., D.Sc. (Centre of New Technologies and the Division of Biophysics, Faculty of

Physics, University of Warsaw, Warsaw, Poland) for insightful discussion of nucleic acid interactions, and Dr. P. Zaleski-Ejgierd (IPC PAS, Warsaw, Poland) for guidance and valuable discussion on ab-initio computations. We are also thankful to M.Sc. Karolina Golebiewska (IPC PAS, Warsaw, Poland) for AFM imaging, Dr. Pawel Borowicz (IPC PAS, Warsaw, Poland) for PM-IRRAS spectra measuring, Dr. M. Cieplak for artwork of Schemes 1 and S1, Dr. M. Wszelaka-Rylik (IPC PAS, Warsaw, Poland) for assistance in the isothermal titration calorimetry experiments, and M.Sc. G. Witkowski (IOC PAS, Warsaw, Poland) for synthesis of the thymine appended functional monomer **4**. The Parent-Bridge Programme (Grant No. POMOST/2012-6/10 to A.P.-L.) of the Foundation for Polish Science (FPS), co-financed by European Union Regional Development Fund, the Polish National Science Centre (NCN, Grant No. 2014/15/B/NZ7/01011 to W.K.), and the U.S. National Science Foundation (Grant CHE-1401188 to F.D.) financially supported the present research.

REFERENCES

(1) Watson, J. D.; Crick, F. H. C., Genetical implications of the structure of deoxyribonucleic acid. *Nature* **1953,** *171*, 964-967.
(2) Watson, J. D.; Crick, F. H. C., Molecular structure of nucleic acids: A structure for deoxyribose nucleic acid. *Nature* **1953,** *171*, 737-738.
(3) Ballard, D. G. H.; Bamford, C. H., Studies in polymerization. X. 'The Chain-Effect'. *Proc. R. Soc. Lond. A* **1956,** *A236*, 384-396.
(4) Li, X.; Zhan, Z.-Y. J.; Knipe, R.; Lynn, D. G., DNA-catalyzed polymerization. *J. Am. Chem. Soc.* **2002,** *124*, 746-747.
(5) Schomaker, E.; Ten Brinke, G.; Challa, G., Complexation of stereoregular poly(methyl methacrylates). 8. Calorimetric investigations. *Macromolecules* **1985,** *18*, 1930-1937.
(6) Naylor, R.; Gilham, P. T., Studies on some interactions and reactions of oligonucleotides in aqueous solution. *Biochemistry* **1966,** *5*, 2722-2728.
(7) Datta, B.; Schuster, G. B., DNA-directed synthesis of aniline and 4-aminobiphenyl oligomers: programmed transfer of sequence information to a conjoined polymer nanowire. *J. Am. Chem. Soc.* **2008,** *130*, 2965-2973.
(8) Aldaye, F. A.; Palmer, A. L.; Sleiman, H. F., Assembling materials with DNA as the guide. *Science* **2008,** *321*, 1795-1799.
(9) Silverman, A. P.; Kool, E. T., Detecting RNA and DNA with templated chemical reactions. *Chem. Rev.* **2006,** *106*, 3775-3789.

(10) Taillon-Miller, P.; Zhijie Gu, Z.; Qun Li; Hillier, L.; Kwok, P.-Y., Overlapping genomic sequences: A treasure trove of single-nucleotide polymorphisms. *Genome Res.* **1998,** *8*, 748-754.
(11) Jorde, L. B., Linkage disequilibrium and the search for complex disease genes. *Genome Res.* **2000,** *10*, 1435-1444.
(12) Gray, I. C.; Cambell, D. A.; Spurr, N. K., Single nucleotide polymorphisms as tools in human genetics. *Hum. Mol. Gen.* **2000,** *9*, 2403-2408.
(13) Kirk, B. W.; Feinsod, M.; Favis, R.; Kliman, R. M.; Barany, F., Single nucleotide polymorphism seeking long term association with complex disease. *Nucleic Acids Res.* **2002,** *30*, 3295-3311.
(14) Bichenkova, E. V.; Lang, Z.; Yu, X.; Rogert, C.; Douglas, K. T., DNA-mounted self-assembly: New approaches for genomic analysis and SNP detection. *Biochim. Biophys. Acta, Gene Regul. Mech.* **2011,** *1809*, 1-23.
(15) He, Y. Q.; Zeng, K.; Gurung, A. S.; Baloda, M.; Xu, H.; Zhang, X. B.; Liu, G. D., Visual detection of single-nucleotide polymorphism with hairpin oligonucleotide-functionalized gold nanoparticles. *Anal. Chem.* **2010,** *82*, 7169-7177.
(16) Kolpashchikov, D. M., Split DNA enzyme for visual single nucleotide polymorphism typing. *J. Am. Chem. Soc.* **2008,** *130*, 2934-2935.
(17) Kolpashchikov, D. M., A binary DNA probe for highly specific nucleic acid recognition. *J. Am. Chem. Soc.* **2006,** *128*, 10625-10628.
(18) Xiang, Y.; Deng, K.; Xia, H.; Yao, C. Y.; Chen, Q. H.; Zhang, L. Q.; Liu, Z. Y.; Fu, W. L., Isothermal detection of multiple point mutations by a surface plasmon resonance biosensor with Au nanoparticles enhanced surface-anchored rolling circle amplification. *Biosens. Bioelectron.* **2013,** *49*, 442-449.
(19) Gao, F. L.; Zhu, Z.; Lei, J. P.; Geng, Y.; Ju, H. X., Sub-femtomolar electrochemical detection of DNA using surface circular strand-replacement polymerization and gold nanoparticle catalyzed silver deposition for signal amplification. *Biosens. Bioelectron.* **2013,** *39*, 199-203.
(20) Hu, Q.; Hu, W. W.; Kong, J. M.; Zhang, X. J., Ultrasensitive electrochemical DNA biosensor by exploiting hematin as efficient biomimetic catalyst toward in situ metallization. *Biosens. Bioelectron.* **2015,** *63*, 269-275.
(21) Nguyen, A. H.; Sim, S. J., Nanoplasmonic biosensor: Detection and amplification of dual bio-signatures of circulating tumor DNA. *Biosen. Bioelectron.* **2015,** *67*, 443-449.
(22) Wang, K.; Sun, Z.; Feng, M.; Liu, A.; Yang, S.; Chen, Y.; Lin, X., Design of a sandwich-mode amperometric biosensor for detection of PML/RARα fusion gene using locked nucleic acids on gold electrode. *Biosens. Bioelectron.* **2011**, 2870-2876.
(23) Wang, Y. X.; Chen, M.; Zhang, L. Q.; Ding, Y.; Luo, Y.; Xu, Q. H.; Shi, J. F.; Cao, L.; Fu, W. L., Rapid detection of human papilloma virus using a novel leaky surface acoustic wave peptide nucleic acid biosensor. *Biosens. Bioelectron.* **2009,** *24*, 3455-3460.
(24) Simeonov, A.; Nikiforov, T. T., Single nucleotide polymorphism genotyping using short, fluorescently labeled locked nucleic acid (LNA) probes and fluorescence polarization detection. *Nucleic Acids Res.* **2002,** *30*, e91-e91.
(25) Stein, C. A., Two problems in antisense biotechnology: In vitro delivery and the design of antisense experiments. *Biochim. Biophys. Acta, Gene Struct. Expression* **1999,** *1489*, 45-52.

(26) Petersen, M.; Wengel, J., LNA: a versatile tool for therapeutics and genomics. *Trends Biotechnol.* **2003,** *21*, 74-81.
(27) Miotke L., M. A., Ji H., Brewer J., Astakhova K., Enzyme-free detection of mutations in cancer DNA using synthetic oligonucleotide probes and fluorescence microscopy. *PLoS One* **2015,** *10*, e0136720.
(28) Fotin A.V., D. A. L., Proudnikov D.Y., Perov A.N., Mirzabekov A.D., Parallel thermodynamic analysis of duplexes on oligodeoxyribonucleotide microchips. *Nucleic Acids Res.* **1998,** *26*, 1515-1521.
(29) Loakes, D., Survey and summary: The applications of universal DNA base analogues. *Nucleic Acids Res.* **2001,** *29*, 2437-2447.
(30) Yang, C.; Bolotin, E.; Jiang, T.; Sladek, F. M.; Martinez, E., Prevalence of the initiator over the TATA box in human and yeast genes and identification of DNA motifs enriched in human TATA-less core promoters. *Gene* **2007,** *389*, 52-65.
(31) Huynh, T.-P.; Pietrzyk-Le, A.; KC, C. B.; Noworyta, K. R.; Sobczak, J. W.; Sharma, P. S.; D'Souza, F.; Kutner, W., Electrochemically synthesized molecularly imprinted polymer of thiophene derivatives for flow-injection analysis determination of adenosine-5′-triphosphate (ATP). *Biosens. Bioelectron.* **2013,** *41*, 634-641.
(32) Sharma, P. S.; Pietrzyk-Le, A.; D'Souza, F.; Kutner, W., Electrochemically synthesized polymers in molecular imprinting for chemical sensing. *Anal. Bioanal. Chem.* **2012,** *402*, 3177-3204.
(33) Sannicolò, F.; Rizzo, S.; Benincori, T.; Kutner, W.; Noworyta, K.; Sobczak, J. W.; Bonometti, V.; Falciola, L.; Mussini, P. R.; Pierini, M., An effective multipurpose building block for 3D electropolymerisation 2,2 '-Bis(2,2 '-bithiophene-5-yl)-3,3 '-bithianaphthene. *Electrochim. Acta* **2010,** *55*, 8352-8364.
(34) Malitesta, C.; Mazzotta, E.; Picca, R. A.; Poma, A.; Chianella, I.; Piletsky, S. A., MIP sensors - the electrochemical approach. *Anal. Bioanal. Chem.* **2012,** *402*, 1827-1846.
(35) Yarman, A.; Scheller, F. W., Coupling biocatalysis with molecular imprinting in a biomimetic sensor. *Angew. Chem.* **2013,** *125*, 11735-11739.
(36) Hvastkovs, E. G.; Buttry, D. A., Recent advances in electrochemical DNA hybridization sensors. *Analyst* **2010,** *135*, 1817-1829.
(37) Li, S.; Cao, S.; Whitcombe, M. J.; Piletsky, S. A., Size matters: Challenges in imprinting macromolecules. *Prog. Polym. Sci.* **2014,** *39*, 145-163.
(38) Zhang, Z.; Liu, J., Molecularly imprinted polymers with DNA aptamer fragments as macromonomers. *ACS Appl. Mater. Interfaces* **2016,** *8*, 6371–6378.
(39) Shea, K. J.; Spivak, D. A.; Sellergen, B., Polymer complements to nucleotide bases - selective binding of adenine- derivatives to imprinted polymers *J. Am. Chem. Soc.* **1993,** *115*, 3368-3369.
(40) Spivak, D.; Gilmore, M. A.; Shea, K. J., Evaluation of binding and origins of specificity of 9-ethyladenine imprinted polymers. *J. Am. Chem. Soc.* **1997,** *119*, 4388-4393.
(41) Tiwari, A.; Deshpande, S.; Kobayashi, H.; Turner, A. P. F., Detection of p53 gene point mutation using sequence-specific molecularly imprinted PoPD electrode. *Biosens. Bioelectron.* **2012,** *35*, 224-229.
(42) Slinchenko, O.; Rachkov, A.; Miyachi, H.; Ogiso, M.; Minoura, N., Imprinted polymer layer for recognizing double-stranded DNA. *Biosens. Bioelectron.* **2004,** *20*, 1091-1097.
(43) Karlsson, B. C. G.; O'Mahony, J.; Karlsson, J. G.; Bengtsson, H.; Eriksson, l. A.; Nicholls, I. A., Structure and dynamics of monomer template complexation: An explanation for

molecularly imprinted polymer recognition site heterogeneity. *J. Am. Chem. Soc.* **2009,** *131*, 13297-13304.

(44) Furche, F.; Ahlrichs, R.; Hattig, C.; Klopper, W.; Sierka, M.; Weigend, F., Turbomole. *WIREs Comput. Mol. Sci.* **2014,** *4*, 91-100.

(45) Cybulski, S. M.; Bledson, T. M.; Toczydlowski, R. R., Comment on hydrogen bonding and stacking interactions of nucleic acid base pairs: A density-functional-theory treatment. *J. Chem. Phys.* **2002,** *116*, 11039-11040.

(46) Elstner, M.; Hobza, P.; Frauenheim, T.; Suhai, S.; Kaxiras, E., Hydrogen bonding and stacking interactions of nucleic acid base pairs: A density-functional-theory based treatment. *J. Chem. Phys.* **2001,** *114*, 5149-5155.

(47) Hobza, P.; Šponer, J., Toward true DNA base-stacking energies: MP2, CCSD(T), and complete basis set calculations. *J. Am. Chem. Soc.* **2002,** *124*, 11802–11808.

(48) Graziano, G.; Klimeš, J.; Fernandez-Alonso, F.; Michaelides, A., Improved description of soft layered materials with van der Waals density functional theory. *J. Phys. Condens. Matter.* **2012,** *24*, 424216-424223.

(49) Sen, A.; Nielsen, P. E., On the stability of peptide nucleic acid duplexes in the presence of organic solvents. *Nucl. Acids Res.* **2007,** *35*, 3367-3374.

(50) Egholm, M.; Buchardt, O.; Christensen, L.; Behrens, C.; Freier, S. M.; Driver, D. A.; Berg, R. H.; Kim, S. K.; Norden, B.; Nielsen, P. E., PNA hybridizes to complementary oligonucleotides obeying the Watson–Crick hydrogen-bonding rules. *Nature* **1993,** *365*, 566-568.

(51) Miyamoto, K.-I.; Ishibashi, K.-I.; Yamaguchi, R.-T.; Kimura, Y.; Ishii, H.; Niwano, M., In situ observation of DNA hybridization and denaturation by surface infrared spectroscopy. *J. Appl. Phys.* **2006,** *99*, 094702-7.

(52) Socrates, G., *Infrared and raman characteristic group frequencies*. 3 ed.; Wiley: New York, 2001.

(53) Pietrzyk-Le, A.; D'Souza, F.; Kutner, W., Applications of supramolecular self-assembly governed molecularly imprinted polymers for selective chemical sensing. In *Supramolecular Chemistry for 21st Century Technology*, Schneider, H.-J., Ed. Taylor & Francis/CRC Press: Boca Raton London New York, UK, 2012, pp. 105-128.

(54) Spivak, D. A.; Shea, K. J., Investigation into the scope and limitations of molecular imprinting with DNA molecules. *Anal. Chim. Acta* **2001,** *435*, 65-74.

(55) Ratautaite, V.; Topkaya, S. N.; Mikoliunaite, L.; Ozsos, M.; Oztekin, Y., Molecularly imprinted polypyrrole for DNA determination. *Electroanalysis* **2013,** *25*, 1169-1177.

(56) Dragulescu-Andrasi, A.; Rapireddy, S.; Frezza, B. M.; Gayathri, C.; Gil, R. R.; Ly, D. H., A simple γ-backbone modification preorganizes peptide nucleic acid into a helical structure. *J. Am. Chem. Soc.* **2006,** *128*, 10258-10267.

(57) Nielsen, P. E.; Egholm, M.; Berg, R. H.; Buchardt, O., Sequence-selective recognition of DNA by strand displacement with a thymine-substituted polyamide. *Science* **1991,** *254*, 1497-1500.

(58) Dueholm, K. L.; Petersen, K. H.; Jensen, D. K.; Egholm, M.; Nielsen, P. E.; Buchardt, O., Peptide nucleic acid (PNA) with a chiral backbone based on alanine. *Bioorg. Med. Chem. Lett.* **1994,** *4*, 1077-1080.

(59) Naumkin, A. V.; Kraut-Vass, A.; Gaarenstroom, S. W.; Powell, C. J. *NIST X-ray Photoelectron Spectroscopy Database 20*, Version 4.1.; 2012.

(60) Pietrzyk, A.; Kutner, W.; Chitta, R.; Zandler, M. E.; D'Souza, F.; Sannicolo, F.; Mussini, P. R., Melamine acoustic chemosensor based on molecularly imprinted polymer film. *Anal. Chem.* **2009,** *81*, 10061-10070.
(61) Skladal, P., Piezoelectric quartz crystal sensors applied for bioanalytical assays and characterization of affinity interactions. *J. Braz. Chem. Soc.* **2003,** *14*, 491-502.
(62) Šípová, H.; Vrba, D.; Homola, J., Analytical value of detecting an individual molecular binding event: The case of the surface plasmon resonance biosensor. *Anal. Chem.* **2012,** *84*, 30-33.
(63) Marshall, K. A.; Robertson, M. P.; Ellington, A. D., A biopolymer by any other name would bind as well: a comparison of the ligand-binding pockets of nucleic acids and proteins. *Structure* **1997,** *5*, 729-734.
(64) Mateo-Martí, E.; Pradier, C.-M., A novel type of nucleic acid-based biosensors: The use of PNA probes, associated with surface science and electrochemical detection techniques. In *Intelligent and Biosensors*, Somerset, V. S., Ed. INTECH, Croatia: 2010; pp 323-344.
(65) Schwarz, F. P.; Robinson, S.; Butler, J. M., Thermodynamic comparison of PNA/DNA and DNA/DNA hybridization reactions at ambient temperature. *Nucleic Acids Res.* **1999,** *27*, 4792-4800.
(66) Cattani-Scholz, A.; Pedone, D.; Blobner, F.; Abstreiter, G.; Schwartz, J.; Tornow, M.; Andruzzi, L., PNA-PEG modified silicon platforms as functional bio-interfaces for applications in DNA microarrays and biosensors. *Biomacromolecules* **2009,** *10*, 489-496.
(67) Weiler, J.; Gausepohl, H.; Hauser, N.; Jensen, O. N.; Hoheisel, J. r. D., Hybridisation based DNA screening on peptide nucleic acid (PNA) oligomer arrays. *Nucleic Acids Res.* **1997,** *25*, 2792-2799.
(68) De, A.; Souchelnytskyi, S.; van den Berg, A.; Carlen, E. T., Peptide nucleic acid (PNA)-DNA duplexes: comparison of hybridization affinity between vertically and horizontally tethered PNA probes. *ACS Appl. Mater. Interfaces* **2013,** *5*, 4607-4612.
(69) Wilson, I. G., Inhibition and facilitation of nucleic acid amplification. *App. Environ. Microbiol.* **1997,** *63*, 3741-3751.
(70) Pietrzyk, A.; Kutner, W.; Chitta, R.; Zandler, M. E.; D'Souza, F.; Sannicolo, F.; Mussini, P. R., *Anal. Chem.* **2009,** *81*, 10061-10070.
(71) Toye, B.; Woods, W.; Bobrowska, M.; Ramotar, K., Inhibition of PCR in genital and urine specimens submitted for Chlamydia trachomatis testing. *J. Clin. Microbiol.* **1998,** *36*, 2356-2358.
(72) Wiedbrauk, D. L.; Werner, J. C.; Drevon, A. M., Inhibition of PCR by aqueous and vitreous fluids. *J. Clin. Microbiol.* **1995,** *33*, 2643-2646.
(73) Rodriguez, R. A.; Thie, L.; Gibbons, C. D.; Sobsey, M. D., Reducing the effects of environmental inhibition in quantitative real-time PCR detection of adenovirus and norovirus in recreational seawaters. *J. Virological Methods* **2012,** *181*, 43-50.
(74) Rossen, L.; Norskov, P.; Holmstrom, K.; Rasmussen, O. F., Inhibition of PCR by components of food samples, microbial diagnostic assays and DNA-extraction solutions. *Int. J. Food Microbiol.* **1992,** *17*, 37-45.
(75) Alaeddini, R., Forensic implications of PCR inhibition-A review. *Forensic Science International-Genetics* **2012,** *6*, 297-305.
(76) Mullis, K. B.; Faloona, F. A., Specific synthesis of DNA invitro via a polymerase-catalyzed chain-reaction. *Methods Enzymol.* **1987,** *155*, 335-350.

(77) Song, L. A.; Shan, D. D.; Zhao, M. W.; Pink, B. A.; Minnehan, K. A.; York, L.; Gardel, M.; Sullivan, S.; Phillips, A. F.; Hayman, R. B.; Walt, D. R.; Duffy, D. C., Direct detection of bacterial genomic DNA at sub-femtomolar concentrations using single molecule arrays. *Anal. Chem.* **2013,** *85*, 1932-1939.